Carbohydrate Polymers Volume 92, Issue 2, 15 February 2013, Pages 1767–1775

http://dx.doi.org/10.1016/j.carbpol.2012.11.006

http://www.sciencedirect.com/science/article/pii/S0144861712011095#

BIOCOMPOSITE FROM POLYLACTIC ACID AND LIGNOCELLULOSIC FIBERS: STRUCTURE-PROPERTY CORRELATIONS

G. Faludi[1,2], G. Dora[1,2], K. Renner[1,2], J. Móczó[1,2,*] and B. Pukánszky[1,2]

[1]Laboratory of Plastics and Rubber Technology, Department of Physical Chemistry and Materials Science, Budapest University of Technology and Economics, H-1521 Budapest, P.O. Box 91, Hungary

[2]Institute of Materials and Environmental Chemistry, Research Center for Natural Sciences, Hungarian Academy of Sciences, H-1525 Budapest, P.O. Box 17, Hungary

*Corresponding author: Phone: +36-1-463-3477, Fax: +36-1-463-3474, Email: jmoczo@mail.bme.hu

ABSTRACT

PLA biocomposites were prepared using three corncob fractions and a wood fiber as reference. The composites were characterized by tensile testing, scanning electron (SEM) and polarization optical (POM) microscopy. Micromechanical deformation processes were followed by acoustic emission measurements. The different strength of the components was proved by direct measurements. Two consecutive micromechanical deformation processes were detected in composites containing the heavy fraction of corncob, which were assigned to the fracture of soft and hard particles, respectively. The fracture of soft particles does not result in the failure of the composites that is initiated either by the fracture of hard particles or by matrix cracking. Very large particles debond easily from the matrix resulting in catastrophic failure at very low stresses. At sufficiently large shear stresses large particles break easily during compounding, thus reinforcement depending on interfacial adhesion was practically the same in all composites irrespectively of initial fiber characteristics.

KEYWORDS: PLA/wood biocomposites, agricultural waste, fiber structure, local deformations, failure mechanism

1. INTRODUCTION

Biodegradable and compostable materials are produced and used in increasing amounts in several areas of life. Biodegradable polymers can be applied in packaging and agriculture, but the application range of compostable materials, including PLA, is even wider, it extends from the electronic to the automotive industry, but it can be used also in construction (Ogawa & Obuchi 2010). Often large stiffness and strength is required from structural materials, thus PLA is often modified with inorganic fillers (Chang et al. 2003; Fukushima et al. 2010; Fukushima et al. 2009; Huda et al. 2007; Imre et al. 2012; Jiang et al. 2007; Kasuga et al. 2003; Kim et al. 2010; Li et al. 2009; Li et al. 2008; Lin et al. 2007; Luo et al. 2009; Marras et al. 2007; Molnár et al. 2009;

Murariu et al. 2008; Nakayama & Hayashi 2007; Rhim et al. 2009; Russias et al. 2006; Wang et al. 2010; Yuzay et al. 2010) and with fibers (Ahmed et al. 2011; Chen et al. 2010; Haque et al. 2010; Huda et al. 2006b; Liu et al. 2012; Shen et al. 2009; Wan et al. 2001). The combination of PLA with natural fibers is a convenient way to produce compostable material thus the study of the structure and properties of such composites is of large scientific and practical interest (Bax & Müssig 2008; Bledzki et al. 2009; Huda et al. 2006a; Huda et al. 2008; Huda et al. 2005; Mathew et al. 2005; Oksman et al. 2003; Petersson et al. 2007; Petinakis et al. 2009; Plackett et al. 2003; Suryanegara et al. 2009; Sykacek et al. 2009; Van de Velde & Kiekens 2002).

The properties of all heterogeneous materials are determined by component properties, composition, structure and interfacial interactions. Interfacial adhesion is a contradictory issue in PLA/natural fiber composites. Some sources claim the formation of strong interaction between the fiber and PLA, while others state that interfacial interactions are weak in these materials. The controversy is demonstrated well also by the occasional contradiction within the same paper. Plackett (Plackett et al. 2003) for example observed the increase of strength in PLA containing 40 wt% jute fabric compared to that of the neat matrix and explained it with good adhesion. On the other hand, he found voids around the fibers on SEM micrographs and concluded that adhesion must be improved. Similarly, Huda et al. (Huda et al. 2006a) deduced from the analysis of stiffness that interfacial adhesion is weak, but based on SEM micrographs they reasoned that adhesion must be strong, since no debonding was observed at the matrix/fiber interface and failure was caused by matrix fracture. However, the analysis of papers available for us show that based on their results most authors arrived to the conclusion that the interaction between PLA and lignocellulosic fibers is weak (Bax & Müssig 2008; Bledzki et al. 2009; Huda et al. 2006a; Huda et al. 2005; Mathew et al. 2005; Oksman et al. 2003; Petinakis et al. 2009; Plackett et al. 2003; Sykacek et al. 2009).

In a previous work we prepared PLA composites using six lignocellulosic fibers with widely varying particle characteristics (Dora et al. 2012). The six fibers included four wood flours from different sources and with dissimilar pre-treatment, microcrystal-

line cellulose and corn cob. We estimated interfacial adhesion with three independent methods and contrary to most claims published in the literature found that interfacial adhesion between PLA and natural fibers is rather strong. Both acoustic emission measurements and microscopy indicated that the dominating micromechanical deformation process is the fracture of the fibers and close correlation was found between the initiation stress of fiber fracture, reinforcement and the ultimate strength of the composites. Corn cob behaved differently from the rest of the reinforcements used, at least two consecutive deformation processes were detected during the loading of composites containing this filler. We could not find a plausible explanation for this behavior, but assumed that the dissimilar inherent structure of corn cob compared to other wood and cellulose samples gives rise to an additional deformation process besides fiber fracture. This latter can be debonding, fiber pull-out, but it can result also from the different strength and fracture of the various parts of the filler.

The study of a considerable number of published papers indicated that the structure of the reinforcement is rarely considered in polymer/lignocellulosic fiber composites, although it might influence deformation mechanism and overall properties. As a consequence, the goal of our work was to investigate this question more in detail. Three different corn cobs with dissimilar structure and properties were acquired and PLA composites were prepared in a wide composition range. A commercially available wood fiber was used as reference. Special attention was paid to micromechanical deformations, reinforcement and the effect of fiber characteristics on the failure mechanism and properties of the composites.

2. EXPERIMENTAL

The PLA used in the experiments was obtained from NatureWorks (USA). The selected grade (Ingeo 4032D, M_n = 88500 g/mol and M_w/M_n = 1.8) is recommended for extrusion. The polymer (<2% D isomer) has a density of 1.24 g/cm^3, while its MFI is 3.9 g/10 min at 190 °C and 2.16 kg load. Three corn cob fillers and a wood fiber (Filtracel EFC 1000, J. Rettenmaier & Söhne GmbH, Germany) were used as rein-

forcements in the study. The particle characteristics and strength of the fibers will be discussed later in detail (see section 3.1).

Both poly(lactic acid) and the fibers were dried in a vacuum oven before composite preparation (110 °C for 4 hours and 105 °C for 4 hours, respectively). The components were homogenized using a Brabender W 50 EHT internal mixer at 180 °C, 50 rpm for 10 min. Wood content changed in a relative wide range, composites contained 5, 10, 15, 20, 30, 40, 50 and 60 vol% lignocellulosic fibers. The homogenized material was compression molded to 1 mm thick plates at 190 °C using a Fontijne SRA 100 machine. All specimens were kept in a room with controlled temperature and humidity (23 °C and 50 %) for at least two weeks prior further testing.

Mechanical properties were characterized by the tensile testing of specimens cut from the 1 mm thick plates using an Instron 5566 apparatus. The measurements were done at 5 mm/min cross-head speed and 115 mm gauge length. Micromechanical deformation processes were followed by acoustic emission (AE) measurements. A Sensophone AED 40/4 apparatus was used to record and analyze acoustic signals during tensile tests. The particle characteristics of the fibers and the structure, as well as the deformation mechanism of the composites were studied by scanning electron microscopy, SEM (JEOL JSM-6380 LA). Micrographs were recorded on tensile fracture surfaces. Failure mechanism was studied also on model composites by polarization optical microscopy (POM). Thin (about 200 μm) films were compression molded from the composites, fractured by tensile testing and the broken halves were studied in the microscope to determine failure mode and the role of the fiber in it.

3. RESULTS AND DISCUSSION

The morphology of PLA/lignocellulosic composites can be relatively complicated. The polymer can crystallize, but the rate of crystallization is rather slow thus under the conditions of normal processing operations it remains mostly amorphous. Besides crystalline structure the possible formation of aggregates, especially at large fiber loadings, is also an important issue. The fiber might influence also interphase formation and

the mobility of the polymer molecules. We investigated these questions in previous studies in detail (Dora et al. 2012; Imre et al. 2012; Molnár et al. 2009). We found that crystallinity is negligible in PLA, while in PP/wood composites limited aggregation resulted from the mere physical contact of the particles due to geometrical reasons (Dányádi et al. 2007). As a consequence we refrain from the detailed discussion of matrix and composite structure and focus mostly on fiber structure, micromechanical deformations, and failure mechanism. Consequences for practice are discussed in the final section of the paper.

3.1. Fiber structure and properties

The structure of corn cob is rather complex. As shown in Fig. 1 it consists of four components. The external parts are the beeswing (1) and the chaff (2) followed by a woody ring (3). The core of the cob is the pith (4), which has completely different properties from the rest. Corn cob is utilized for several purposes like cleaning of metal parts, surface polishing, as additive for cleaning material, pet litter, carrier for fodder, but also as reinforcing fiber, e.g. in extruded PVC insulating sheets. Before use corn cob is ground and separated to two fractions, a *heavy* and a *light* part. The *heavy* fraction contains *hard* while *light fraction* consist mostly of *soft particles*. The properties of the two fractions differ from each other. In order to study the effect of the various parts of corn cob on composite properties we obtained both the *heavy* and the *light fraction* from the producer. Moreover, since the particle size of the *light fraction* was much larger than that of the *hard particles*, at least it contained quite a few very large particles, we ground the *light fraction* to smaller particle size. Accordingly, four fillers were compared in this study: the reference wood fiber, the *heavy* and *light fractions* of corn cob and the *ground light fraction* (abbreviated as *gsoft* in tables and text).

Since in earlier studies (Dora et al. 2012; Renner et al. 2010a; Renner et al. 2009) we found that the particle characteristics of lignocellulosic fibers influence composite properties significantly they were analyzed quite thoroughly. Particle characteristics were determined quantitatively by laser light scattering. The particle size distribu-

tion of the four fillers studied is presented in Fig. 2. The particle size of the *light* (*soft*) *fraction* is the largest as expected, while the *ground light fraction* (*gsoft*) contains the smallest particles. Particle size distributions differ considerably; the bimodal distribution of the *ground light fraction* indicates particles with dissimilar properties. We may assume that the separation of the *heavy* and *light fractions* was not perfect during the production of the fibers. Since lignocellulosic fibers are usually anisotropic, further characterization was done by the image analysis of SEM micrographs in order to obtain information also about length, diameter and aspect ratio. The results are compiled in Table 1. In earlier studies (Renner et al. 2010a; Renner et al. 2009) we found that aspect ratio is one of the most important characteristics determining composite properties, however, it is very similar for the three corn cob samples and only slightly larger for the wood flour used.

We may assume that the strength of the various components differ considerably from each other. We made an attempt to measure the inherent strength of the fibers. It was relatively easy to machine specimens from a pine plank, but the separation of the components of corn cob turned out to be impossible. We could cut specimens including all components from dry cobs and we carried out tensile measurements on them in two directions, along the length of the cob and perpendicularly to it. In order to assess the contribution of the components to overall strength we calculated tensile strength in three different ways. Assuming that the strength of components differs considerably from each other indeed, we divided tensile force with three different cross-sections: with that of the *hard part* (woody ring, 1 in Fig. 1) that is very thin, with a ring including the external sections (from 1 to 3), but omitting the pith (4), and with the entire cross-section of the specimen including all four sections. The results are collected in Table 2. We can see that the longitudinal strength of pine wood is more than one order of magnitude larger than the strength of corn cob that is not surprising. We can also conclude that the strength of this latter is practically independent of direction. Finally, the *hard part* is stronger than the pith, the strength of which, however, is in the same range as that of wood perpendicularly to the direction of the fibers. Accordingly we may assume that

soft and *hard particles* fracture differently at different external loads. We must also mention here that we tried testing corn cob specimens also by bending, but it turned out to be rather difficult since often radial cracks were initiated in the specimen. These cracks indicate that the failure of the particles must depend both on size and on the direction of the load, i.e. on particle orientation in our case.

3.2. Micromechanical deformations

Because of the dissimilar elastic properties of the matrix polymer and the inclusion, stress concentration develops around this latter in heterogeneous polymers. Local stress maxima initiate local deformation processes some of which are accompanied by acoustic events. Sound waves can be picked up by microphones and the analysis of the signals may yield valuable information about the deformation and failure of the material. The result of an acoustic measurement carried out on a PLA/corn cob composite is presented in Fig. 3a. The composite contained 15 vol% of the *heavy fraction*. Each small circle is an acoustic event, the amplitude of which can be deduced from the right hand axis of the graph. The corresponding stress vs. strain trace is also shown as reference. We can see that significant acoustic activity starts above a certain deformation and that amplitudes cover a wide range. A closer scrutiny also reveals that two group of signals can be distinguished along the deformation axis indicating two consecutive deformation processes. The second process seems to start at around 0.9-1.0 % elongation. Further conclusion is difficult to deduce from individual signals, additional analysis is needed in order to extract more information from the results. The cumulative number of signals is plotted as a function of deformation in Fig. 3b together with the stress vs. strain trace. The two processes can be clearly distinguished in the trace. The first process appears as a step, while the second starts at around 1.0 % elongation as deduced from the evaluation of individual signals above. Based on the two figures one can conclude that the second process starts at larger deformation thus at larger stresses. Also the amplitude of the signals seems to be somewhat larger in the second process indicating larger fracture energy. We may only speculate about the two processes at this point,

they may belong to the fracture of the different fractions assuming that separation was not perfect, but a completely different process, like debonding may also take place during deformation.

The cumulative number of signal vs. elongation correlations are compared in Fig. 3c for the four fibers studied. The traces are quite different from each other. Acoustic activity starts at relatively large elongation in the PLA/wood composite and at a much smaller one in the other three composites. We may assume that the *light fraction* does not contain considerable amount of *hard particles* thus its acoustic activity is related mainly to *soft particles*. The final section of the cumulative number of signal vs. elongation trace of the composite containing the *hard particles* and the trace obtained for the PLA/wood composite are quite similar. We showed earlier that traces of this shape indicate fiber fracture as the dominating deformation process. The first step detected in these composites is more similar to the traces recorded for the composite containing the *light fraction*. Accordingly we may assume at this stage that the two processes occurring in composites prepared with the *heavy fraction* are related to the *hard* and *soft particles*, respectively, i.e. separation was not complete during production. The trace recorded on composites prepared with the *gsoft fiber* resembles traces obtained with *the soft fraction*, but it starts at larger elongation and the number of signals is smaller. We must consider here the fact that both debonding and particle fracture depends also on the size of the particles and the size of *gsoft particles* is significantly smaller than that of the rest. Accordingly we may assume that the same process takes place in composites containing the *soft* and *gsoft particles*, but particle size also plays a role.

The initiation stress of individual processes can be deduced from the cumulative number of signal vs. elongation traces. The method of determination and the characteristic stress values are shown in Fig. 3b. We assigned σ_{AE1} and σ_{AE2} to the two processes discussed above, the first being mainly related to the *soft*, while the second to the *hard particles*.

Characteristic stresses are plotted against fiber content in Fig. 3d**.** It is quite ob-

vious that two micromechanical processes take place during the deformation of the samples indeed and that they are initiated at significantly different stresses. One process dominates in PLA/wood composites and earlier studies indicated that this is related to the fracture of the fibers (Dora et al. 2012). One process occurs also in composites containing the *light fraction*, but this starts at much smaller stresses, on the one hand, and it have not been identified yet, on the other. Both processes can be observed in the two other sets of composites. The second process can be detected only at small fiber contents (5 and 10 vol%) in the *gsoft composites*, while it occurs also at much larger fiber contents in the PLA/*heavy fraction* materials. Only one process could be identified in these latter at large fiber content (40-60 vol%) and based on earlier experience and the shape of the cumulative number of signal vs. elongation traces we identified it as the second process, i.e. the one related to the *hard particles*. However, the position of these points clearly indicates that identification was wrong and acoustic activity is dominated by *soft particles* in these composites. We can safely conclude that *hard* and *soft particles* behave differently during deformation and that acoustic emission is a useful tool to detect the main processes occurring. Further information is needed, though, to identify the processes themselves, although we think that acoustic signals are emitted by the fracture of the particles, which occurs at different loads for *hard* and *soft fibers*.

3.3. Properties and reinforcement

If the characteristics of the fractions differ significantly and they initiate different micromechanical deformation processes, indeed, we expect that composite properties will be also quite dissimilar. The composition dependence of modulus is presented in Fig. 4a. The difference in the stiffness of the four series is negligible, but this is not very surprising. Stiffness is determined at very small, practically zero deformation, and it depends mainly on the volume fraction of the reinforcement. Particle characteristics and interfacial adhesion influence it only very slightly, especially since all fibers have relatively small aspect ratio and the samples were prepared the same way, thus orientation, if any, is also the same.

Much larger differences are expected in composite strength that is plotted against fiber content in Fig. 4b. Although the effect of the fibers differs somewhat indeed, the differences are smaller than expected and not very easy to explain. Tensile strength decreases with increasing fiber content in accordance with previous experience and published papers. Weak interaction was deduced from this decrease in the literature, but in fact comparison to the theoretical minimum [see broken line (Pukánszky 1990)] indicates considerable reinforcement. Reinforcement is the results of relatively strong interaction. Three of the fibers (wood, *heavy* and *gsoft fraction*) have very similar effect on composite strength that is quite surprising since *soft particle* behavior dominated acoustic activity in the latter. This behavior contradicts previous experience showing close correlation between acoustic activity and tensile strength in various composites (Imre et al. 2012; Renner et al. 2010a; Renner et al. 2010b). The composition dependence of the tensile strength of the composites containing the *light fraction* is even more difficult to explain. At small fiber contents composite strength is below the theoretical minimum calculated from the effective load-bearing cross-section of the matrix assuming zero interaction of the components. Such changes in composite properties can occur only if matrix properties are modified and/or the deformation mechanism changes. We have not found any effect of the fibers on matrix properties (crystallization, plasticization) thus we must assume that in PLA/soft fraction composites failure mechanism is different at small filler loadings from that occurring in the rest of the materials including those prepared with the other three fibers. Even more surprising is the fact that at larger fiber contents composite strength runs parallel with the rest of the composites and does not decrease with the same rate as at small fiber loadings. Further information is needed to reveal the reason of this behavior.

The extent of reinforcement can be estimated quantitatively with the help of simple models. The dependence of tensile strength on filler content can be expressed as (Pukánszky 1990)

$$\sigma_T = \sigma_{T0}\,\lambda^n\,\frac{1-\varphi}{1+2.5\varphi}\exp(B\varphi) \qquad (1)$$

where σ_T and σ_{T0} are the true tensile strength ($\sigma_T = \sigma\lambda$ and $\lambda = L/L_0$) of the composite and the matrix, respectively, n is a parameter expressing the strain hardening tendency of the matrix, φ is the volume fraction of the fiber and B is related to its relative load-bearing capacity, i.e. to the extent of reinforcement, which depends, among other factors, also on interfacial adhesion. The theoretical minimum of strength in Fig. 8 was calculated by assuming $B = 0$. We can write Eq. 1 in linear form

$$\ln \sigma_{Tred} = \ln \frac{\sigma_T \left(1 + 2.5\,\varphi\right)}{\lambda^n \left(1 - \varphi\right)} = \ln \sigma_{T0} + B\,\varphi \qquad (2)$$

and the plot of the natural logarithm of reduced tensile strength against fiber content should result in a linear correlation, the slope of which is proportional to the load-bearing capacity of the fiber, i.e. reinforcement.

The strength of the composites is plotted against filler content in the form indicated by Eq. 2 in Fig. 4c. We obtain straight lines indeed three of which run very close together, as expected (compare to Fig. 4b). Also the slope of the lines related to the extent of reinforcement is very similar in each case, which is more surprising. Even more unexpected is the fact that the line obtained for the PLA/*light fraction* composites runs basically parallel to the other three indicating the same extent of reinforcement. The dissimilar intersection shows the modification of matrix properties and/or changing failure mechanism. Reinforcement, i.e. B parameters, is listed in Table 3 for the four series of composites. The table confirms our qualitative evaluation showing very similar reinforcements. Obviously, in spite of the different micromechanical deformation processes taking place consecutively and/or simultaneously in PLA/corn cob composites, reinforcement and composite properties are determined by the same factors in all composites irrespectively of the type of the fiber used. Further considerations are needed to reveal the reason for the observed behavior.

3.4. Discussion and practical consequences

Several of the results presented above apparently contradict each other and previous experience. Acoustic activity and characteristic stresses were shown to be related strongly earlier (Dora et al. 2012; Renner et al. 2010a; Renner et al. 2009). In this case, however, composite strength and especially reinforcement seem to be independent of acoustic activity or the characteristics of the fibers. Strengths, which are smaller than the theoretical value, also need explanation, especially since reinforcement is the same in PLA/*light fraction* composites as in the others. We hoped that microscopy might offer additional evidence for the dominating deformation and failure mechanism and resolve these contradictions.

A SEM micrograph taken from the fracture surface of a PLA/hard fraction composite created during tensile testing is shown in Fig. 5a. We can see the fracture of a corn cob particle, but also some debonding. Particle fracture dominates in the micrographs taken from most composites including those prepared with the *ground soft filler* (Fig. 5b). Fiber fracture is sometimes accompanied by debonding, fiber pull-out or the local yielding of the matrix. The domination of fiber fracture both in PLA/wood and PLA/corn cob composites is confirmed also by polarization optical microscopy (Fig. 5c and d). The micrographs taken from thin, fractured films clearly show that cracks pass through both wood (Fig. 5c) and corn cob (Fig. 5d) particles. In view of these results it is rather surprising that reinforcement is completely independent of the type of fiber used, since both direct measurements (see Table 2) and acoustic activity (Fig. 3c) shows that *soft particles* break at much smaller stresses than *hard* ones.

The contradiction can be resolved if we consider the results presented in Fig. 6. The tensile strength of the composites is plotted against characteristic stresses derived from acoustic emission measurements in the figure. A very close correlation exists between the characteristic stress of the second process, i.e. the fracture of *hard particles*, but practically none between strength and σ_{AE1}. This clearly proves that the fracture of *soft particles* yields acoustic signals, but does not result in the fracture of the composite, while the fracture of *hard particles* leads to the failure of the composite. Obviously

large, *soft particles* can break without initiating catastrophic failure in the PLA composite.

The final question needing explanation is the small strength of PLA/*light fraction* composites and their relatively large reinforcing effect. Strengths, which are smaller than the theoretical value, can be explained with the large size of some of the *soft particles*. This is demonstrated amply by the SEM micrograph presented in Fig. 7. A very large particle occupying approximately half of the cross-section of the sample and oriented perpendicularly to the direction of the load initiated fracture at very small load. Apparently the particle debonded from the matrix on its entire surface leading to immediate failure. The presence of such particles explains the small strength, but not the absence of this phenomenon at larger fiber contents and the strong reinforcement. We must consider here the small strength of *soft particles*. The viscosity of the melt increases with increasing fiber content quite considerably. This results in relatively large shear stresses developing in the melt during homogenization and larger load on the particles. We tried to model this by calculating the work used for the homogenization of the composites during mixing; the obtained values are plotted against fiber content in Fig. 8. Above a certain load the fibers fracture and fiber attrition results in changing actual particle size distribution (see also Fig. 5b), larger strength and reinforcement. Accordingly, fiber characteristics, interfacial adhesion, aspect ratio and orientation must be very similar in all composites thus explaining the similarity in the extent of reinforcement.

4. CONCLUSIONS

Corn cob is used as reinforcement in industrial practice. Its structure is complex and its constituents have dissimilar properties. The different strength of the components was proved by direct measurements and also by the acoustic activity of the PLA composites prepared from the different fractions. Two consecutive micromechanical deformation processes were detected in composites containing the *heavy fraction* of corn cob which were assigned to the fracture of *soft* and *hard particles*. The occurrence of the two processes indicates that the separation of the components is not perfect in the indus-

trial technology used. The fracture of *soft particles* does not result in the failure of the composites that is initiated either by the fracture of *hard particles* or by matrix cracking. Very large particles debond easily from the matrix resulting in catastrophic failure at very low stresses. At sufficiently large shear stresses large *soft particles* break easily during compounding thus, as a consequence of fiber attrition, reinforcement depending on interfacial adhesion was practically the same in all composites irrespectively of initial fiber characteristics.

5. ACKNOWLEDGEMENTS

Boly Zrt. is acknowledged for the donation of the corn cob samples. The authors are indebted to Zsolt László for his help in the determination of the particle characteristics of wood and to Zoltán Link for his help in the preparation and characterization of the composites. The research on heterogeneous polymer systems was financed by the National Scientific Research Fund of Hungary (OTKA Grant No. K 101124) and by the Forbioplast FP7 project of EU (212239); we appreciate the support very much. One of the authors (KR) is grateful also to the János Bolyai Research Scholarship of the Hungarian Academy of Sciences.

6. REFERENCES

Ahmed, I., Jones, I. A., Parsons, A. J., Bernard, J., Farmer, J., Scotchford, C. A., Walker, G. S., & Rudd, C. D. (2011) Composites for bone repair: phosphate glass fibre reinforced PLA with varying fibre architecture. *Journal of Materials Science-Materials in Medicine 22*, 1825-1834.

Bax, B., & Müssig, J. (2008) Impact and tensile properties of PLA/Cordenka and PLA/flax composites. *Composites Science and Technology 68*, 1601-1607.

Bledzki, A. K., Jaszkiewicz, A., & Scherzer, D. (2009) Mechanical properties of PLA composites with man-made cellulose and abaca fibres. *Composites Part A: Applied Science and Manufacturing 40*, 404-412.

Chang, J.-H., An, Y. U., Cho, D., & Giannelis, E. P. (2003) Poly(lactic acid) nanocomposites: comparison of their properties with montmorillonite and synthetic mica (II). *Polymer 44*, 3715-3720.

Chen, X., Li, Y., & Gu, N. (2010) A novel basalt fiber-reinforced polylactic acid composite for hard tissue repair. *Biomedical Materials 5*, 044104.

Dányádi, L., Janecska, T., Szabó, Z., Nagy, G., Móczó, J., & Pukánszky, B. (2007) Wood flour filled PP composites: Compatibilization and adhesion. *Composites Science and Technology 67*, 2838-2846.

Dora, G., Faludi, G., Imre, B., Renner, K., Móczó, J., & Pukánszky, B. (2012) PLA/Lignocelulosic Fiber Composites: Interfacial Adhesion and Failure Mechanism. *Composites Part A, Applied Science and Manufacturing submitted*.

Fukushima, K., Murariu, M., Camino, G., & Dubois, P. (2010) Effect of expanded graphite/layered-silicate clay on thermal, mechanical and fire retardant properties of poly(lactic acid). *Polymer Degradation and Stability 95*, 1063-1076.

Fukushima, K., Tabuani, D., & Camino, G. (2009) Nanocomposites of PLA and PCL based on montmorillonite and sepiolite. *Materials Science and Engineering: C 29*, 1433-1441.

Haque, P., Parsons, A. J., Barker, I. A., Ahmed, I., Irvine, D. J., Walker, G. S., & Rudd, C. D. (2010) Interfacial properties of phosphate glass fibres/PLA composites: Effect of the end functionalities of oligomeric PLA coupling agents. *Composites Science and Technology 70*, 1854-1860.

Huda, M. S., Drzal, L. T., Misra, M., & Mohanty, A. K. (2006a) Wood-fiber-reinforced poly(lactic acid) composites: Evaluation of the physicomechanical and morphological properties. *Journal of Applied Polymer Science 102*, 4856-4869.

Huda, M. S., Drzal, L. T., Mohanty, A. K., & Misra, M. (2006b) Chopped glass and recycled newspaper as reinforcement fibers in injection molded poly(lactic acid) (PLA) composites: A comparative study. *Composites Science and Technology 66*, 1813-1824.

Huda, M. S., Drzal, L. T., Mohanty, A. K., & Misra, M. (2007) The effect of silane

treated- and untreated-talc on the mechanical and physico-mechanical properties of poly(lactic acid)/newspaper fibers/talc hybrid composites. *Composites Part B: Engineering 38*, 367-379.

Huda, M. S., Drzal, L. T., Mohanty, A. K., & Misra, M. (2008) Effect of fiber surface-treatments on the properties of laminated biocomposites from poly(lactic acid) (PLA) and kenaf fibers. *Composites Science and Technology 68*, 424-432.

Huda, M. S., Mohanty, A. K., Drzal, L. T., Schut, E., & Misra, M. (2005) "Green" composites from recycled cellulose and poly(lactic acid): Physico-mechanical and morphological properties evaluation. *Journal of Materials Science 40*, 4221-4229.

Imre, B., Keledi, G., Renner, K., Móczó, J., Murariu, M., Dubois, P., & Pukánszky, B. (2012) Adhesion and micromechanical deformation processes in PLA/$CaSO_4$ composites. *Carbohydrate Polymers 89*, 759-767.

Jiang, L., Zhang, J., & Wolcott, M. P. (2007) Comparison of polylactide/nano-sized calcium carbonate and polylactide/montmorillonite composites: Reinforcing effects and toughening mechanisms. *Polymer 48*, 7632-7644.

Kasuga, T., Maeda, H., Kato, K., Nogami, M., Hata, K.-i., & Ueda, M. (2003) Preparation of poly(lactic acid) composites containing calcium carbonate (vaterite). *Biomaterials 24*, 3247-3253.

Kim, M. W., Song, Y. S., & Youn, J. R. (2010) Effects of interfacial adhesion and crystallization on the thermoresistance of poly(lactic acid)/mica composites. *Composites Part A: Applied Science and Manufacturing 41*, 1817-1822.

Li, B., Dong, F.-X., Wang, X.-L., Yang, J., Wang, D.-Y., & Wang, Y.-Z. (2009) Organically modified rectorite toughened poly(lactic acid): Nanostructures, crystallization and mechanical properties. *European Polymer Journal 45*, 2996-3003.

Li, J., X.L.Lu, & Zheng, Y. F. (2008) Effect of surface modified hydroxyapatite on the tensile property improvement of HA/PLA composite. *Applied Surface Science 255*, 494-497.

Lin, P.-L., Fang, H.-W., Tseng, T., & Lee, W.-H. (2007) Effects of hydroxyapatite dos-

age on mechanical and biological behaviors of polylactic acid composite materials. *Materials Letters 61*, 3009-3013.

Liu, T., Yu, F., Yu, X., Zhao, X., Lu, A., & Wang, J. (2012) Basalt fiber reinforced and elastomer toughened polylactide composites: Mechanical properties, rheology, crystallization, and morphology. *Journal of Applied Polymer Science 125*, 1292-1301.

Luo, Y.-B., Li, W.-D., Wang, X.-L., Xu, D.-Y., & Wang, Y.-Z. (2009) Preparation and properties of nanocomposites based on poly(lactic acid) and functionalized TiO_2. *Acta Materialia 57*, 3182-3191.

Marras, S. I., Zuburtikudis, I., & Panayiotou, C. (2007) Nanostructure vs. microstructure: Morphological and thermomechanical characterization of poly(l-lactic acid)/layered silicate hybrids. *European Polymer Journal 43*, 2191-2206.

Mathew, A. P., Oksman, K., & Sain, M. (2005) Mechanical properties of biodegradable composites from poly lactic acid (PLA) and microcrystalline cellulose (MCC). *Journal of Applied Polymer Science 97*, 2014-2025.

Molnár, K., Móczó, J., Murariu, M., Dubois, P., & Pukánszky, B. (2009) Factors affecting the properties of PLA/$CaSO_4$ composites: homogeneity and interactions. *Express Polymer Letters 3*, 49-61.

Murariu, M., Ferreira, A. D., Pluta, M., Bonnaud, L., Alexandre, M., & Dubois, P. (2008) Polylactide (PLA)-$CaSO_4$ composites toughened with low molecular weight and polymeric ester-like plasticizers and related performances. *European Polymer Journal 44*, 3842-3852.

Nakayama, N., & Hayashi, T. (2007) Preparation and characterization of poly(l-lactic acid)/TiO_2 nanoparticle nanocomposite films with high transparency and efficient photodegradability. *Polymer Degradation and Stability 92*, 1255-1264.

Ogawa, S., & Obuchi, S. (2010) Packaging and Other Commercial Applications. In *Poly(lactic acid): Synthesis, Structures, Properties, Processing, and Applications* (ed. R. Auras, L.-T. Lim, S. Selke & H. Tsuji), pp. 457-467. New Jersey: Wiley.

Oksman, K., Skrifvars, M., & Selin, J.-F. (2003) Natural fibres as reinforcement in polylactic acid (PLA) composites. *Composites Science and Technology 63,* 1317-1324.

Petersson, L., Kvien, I., & Oksman, K. (2007) Structure and thermal properties of poly(lactic acid)/cellulose whiskers nanocomposite materials. *Composites Science and Technology 67,* 2535-2544.

Petinakis, E., Yu, L., Edward, G., Dean, K., Liu, H. S., & Scully, A. D. (2009) Effect of Matrix-Particle Interfacial Adhesion on the Mechanical Properties of Poly(lactic acid)/Wood-Flour Micro-Composites. *Journal of Polymers and the Environment 17,* 83-94.

Plackett, D., Løgstrup Andersen, T., Batsberg Pedersen, W., & Nielsen, L. (2003) Biodegradable composites based on l-polylactide and jute fibres. *Composites Science and Technology 63,* 1287-1296.

Pukánszky, B. (1990) Influence of Interface Interaction on the Ultimate Tensile Properties of Polymer Composites. *Composites 21,* 255-262.

Renner, K., Kenyó, C., Móczó, J., & Pukánszky, B. (2010a) Micromechanical deformation processes in PP/wood composites: Particle characteristics, adhesion, mechanisms. *Composites Part a-Applied Science and Manufacturing 41,* 1653-1661.

Renner, K., Móczó, J., & Pukánszky, B. (2009) Deformation and failure of PP composites reinforced with lignocellulosic fibers: Effect of inherent strength of the particles. *Composites Science and Technology 69,* 1653-1659.

Renner, K., Móczó, J., Suba, P., & Pukánszky, B. (2010b) Micromechanical deformations in PP/lignocellulosic filler composites: Effect of matrix properties. *Composites Science and Technology 70,* 1141-1147.

Rhim, J.-W., Hong, S.-I., & Ha, C.-S. (2009) Tensile, water vapor barrier and antimicrobial properties of PLA/nanoclay composite films. *LWT - Food Science and Technology 42,* 612-617.

Russias, J., Saiz, E., Nalla, R. K., Gryn, K., Ritchie, R. O., & Tomsia, A. P. (2006) Fab-

rication and mechanical properties of PLA/HA composites: A study of in vitro degradation. *Materials Science and Engineering: C 26*, 1289-1295.

Shen, L., Yang, H., Ying, J., Qiao, F., & Peng, M. (2009) Preparation and mechanical properties of carbon fiber reinforced hydroxyapatite/polylactide biocomposites. *Journal of Materials Science-Materials in Medicine 20*, 2259-2265.

Suryanegara, L., Nakagaito, A. N., & Yano, H. (2009) The effect of crystallization of PLA on the thermal and mechanical properties of microfibrillated cellulose-reinforced PLA composites. *Composites Science and Technology 69*, 1187-1192.

Sykacek, E., Hrabalova, M., Frech, H., & Mundigler, N. (2009) Extrusion of five biopolymers reinforced with increasing wood flour concentration on a production machine, injection moulding and mechanical performance. *Composites Part A: Applied Science and Manufacturing 40*, 1272-1282.

Van de Velde, K., & Kiekens, P. (2002) Biopolymers: overview of several properties and consequences on their applications. *Polymer Testing 21*, 433-442.

Wan, Y. Z., Wang, Y. L., Li, Q. Y., & Dong, X. H. (2001) Influence of surface treatment of carbon fibers on interfacial adhesion strength and mechanical properties of PLA-based composites. *Journal of Applied Polymer Science 80*, 367-376.

Wang, X., Song, G., & Lou, T. (2010) Fabrication and characterization of nanocomposite scaffold of PLLA/silane modified hydroxyapatite. *Medical Engineering & Physics 32*, 391-397.

Yuzay, I. E., Auras, R., Soto-Valdez, H., & Selke, S. (2010) Effects of synthetic and natural zeolites on morphology and thermal degradation of poly(lactic acid) composites. *Polymer Degradation and Stability 95*, 1769-1777.

Table 1 Particle characteristics of the studied lignocellulosic fibers

Fiber	Size, D[4,3] (μm)	Length (μm)	Diameter (μm)	Aspect ratio	Surface area (m^2/g)
Wood	213.1	363.4	63.9	6.8	2.00
Hard	143.4	108.1	55.7	2.3	0.86
Soft	517.3	135.5	45.9	3.6	0.89
Gsoft	71.9	52.0	24.1	2.5	1.56

Table 2 Comparison of the strength of wood and various parts of corn cob in two directions

Component	Strength (MPa) in direction	
	Longitudinal	Transverse
Wood (pine)	81.6 ± 17.7	3.8 ± 0.8
Corn cob, total cross-section	4.0 ± 0.3	2.7 ± 0.5
Corn cob, ring	5.0 ± 0.3	5.4 ± 0.9
Corn cob, hard	21.2 ± 1.4	13.5 ± 2.2

Table 3 Reinforcing effect of the studied lignocellulosic fibers in PLA

Fiber	Matrix strength[a] (MPa)	Parameter *B*	R^{2b}
Wood	53.10	2.29	0.9968
Hard	56.79	1.92	0.9933
Soft	38.64	1.93	0.9823
Gsoft	49.13	2.34	0.9972

[a]calculated from the intersection of the $\ln\sigma_{rel}$ vs. φ lines (measured value 57.9 MPa)

[b]determination coefficient showing the goodness of the linear fit

CAPTIONS

Fig. 1 Structural components of corn cob: 1) beeswing, 2) chaff, 3) woody ring, 4) pith.

Fig. 2 Particle size distribution of the studied lignocellulosic fibers.

Fig. 3 Results of the acoustic emission measurements: a) Evolution of acoustic signals during the tensile testing of a PLA/wood composite (15 vol% *heavy fraction*); (o) individual acoustic signals, ——— stress vs. strain trace. b) Cumulative number of signals vs. elongation trace of the composite of Fig. 3a. The corresponding stress vs. strain trace is plotted as reference. Determination of characteristic stresses. c) Comparison of the cumulative number of signal traces for all the PLA/lignocellulosic fiber composites studied; 15 vol% fiber content. d) Composition dependence of the characteristic stresses derived from acoustic emission measurements; effect of fiber type. Symbols: (□) wood, (○) *hard*, (Δ) *soft*, (∇) *gsoft*; empty symbol σ_{AE1}, full symbol σ_{AE2}.

Fig. 4 Mechanical properties, reinforcement: a) Stiffness of PLA/lignocellulosic fiber composites plotted against fiber content. Symbols: (□) wood, (○) *hard*, (Δ) *soft*, (∇) *gsoft*. b) Effect of the type and amount of reinforcement on the tensile strength of PLA/lignocellulosic fiber composites. Symbols: (□) wood, (○) *hard*, (Δ) *soft*, (∇) *gsoft*, ----- theoretical minimum of strength (B = 0 in Eq. 1). c) Reduced tensile strength of PLA/lignocellulosic fiber composites plotted against fiber content according to Eq. 2. Symbols: (□) wood, (○) *hard*, (Δ) *soft*, (∇) *gsoft*.

Fig. 5 Microscopy: a-b) SEM micrographs taken from the fracture surface of a PLA/lignocellulosic fiber composites at 20 vol% fiber content. Fracture surface was created by failure in the tensile test. a) *hard*, b) *ground soft particles*. c-d) Fiber fracture in PLA model composites, POM micrographs. c) wood, d) *light fraction*. The composites contained 5 vol% fiber.

Fig. 6 Correlation between the characteristic stresses of the two micromechanical deformation processes detected by acoustic emission and the ultimate tensile strength of the composites. Symbols: (□) wood, (○) *hard*, (Δ) *soft*, (∇) *gsoft*; empty symbol σ_{AE1}, full symbol σ_{AE2}.

Fig. 7 Debonding of a very large *soft particle* and the catastrophic failure of the composite. The SEM micrograph was taken from fracture surface created in tensile testing. Fiber content: 20 vol%.

Fig. 8 Composition dependence of relative (related to neat PLA) work of compounding put into the homogenization of the composites. Three parallel series prepared with *light particles*.

FIGURES

Faludi, Fig. 1

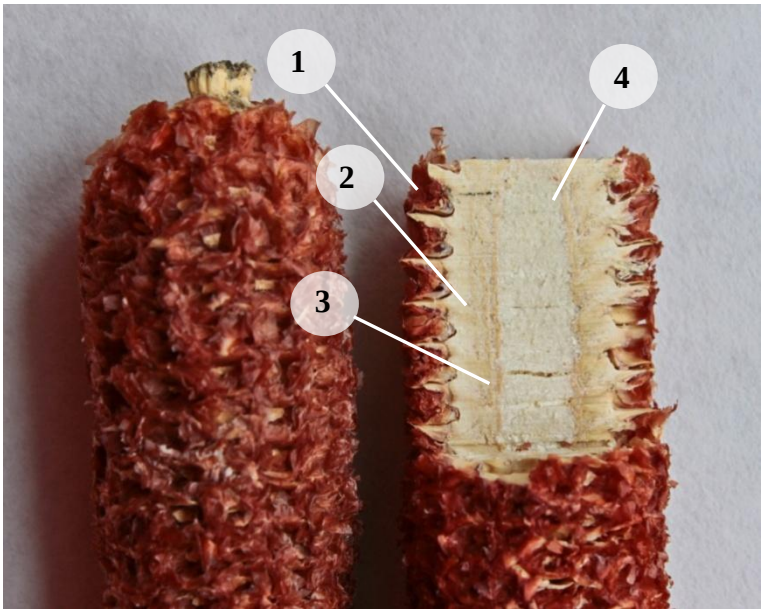

Faludi, Fig. 2

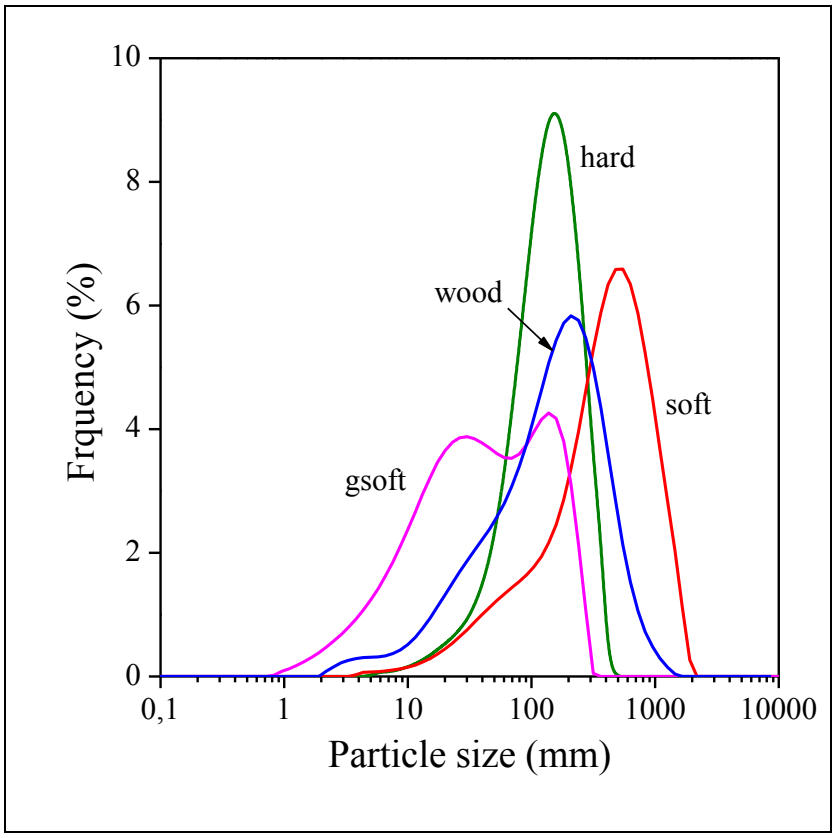
10
8
6
4
2
0
Frquency (%)
hard
wood
soft
gsoft
0,1
1
10
100
1000
10000
Particle size (mm)

Faludi, Fig. 3

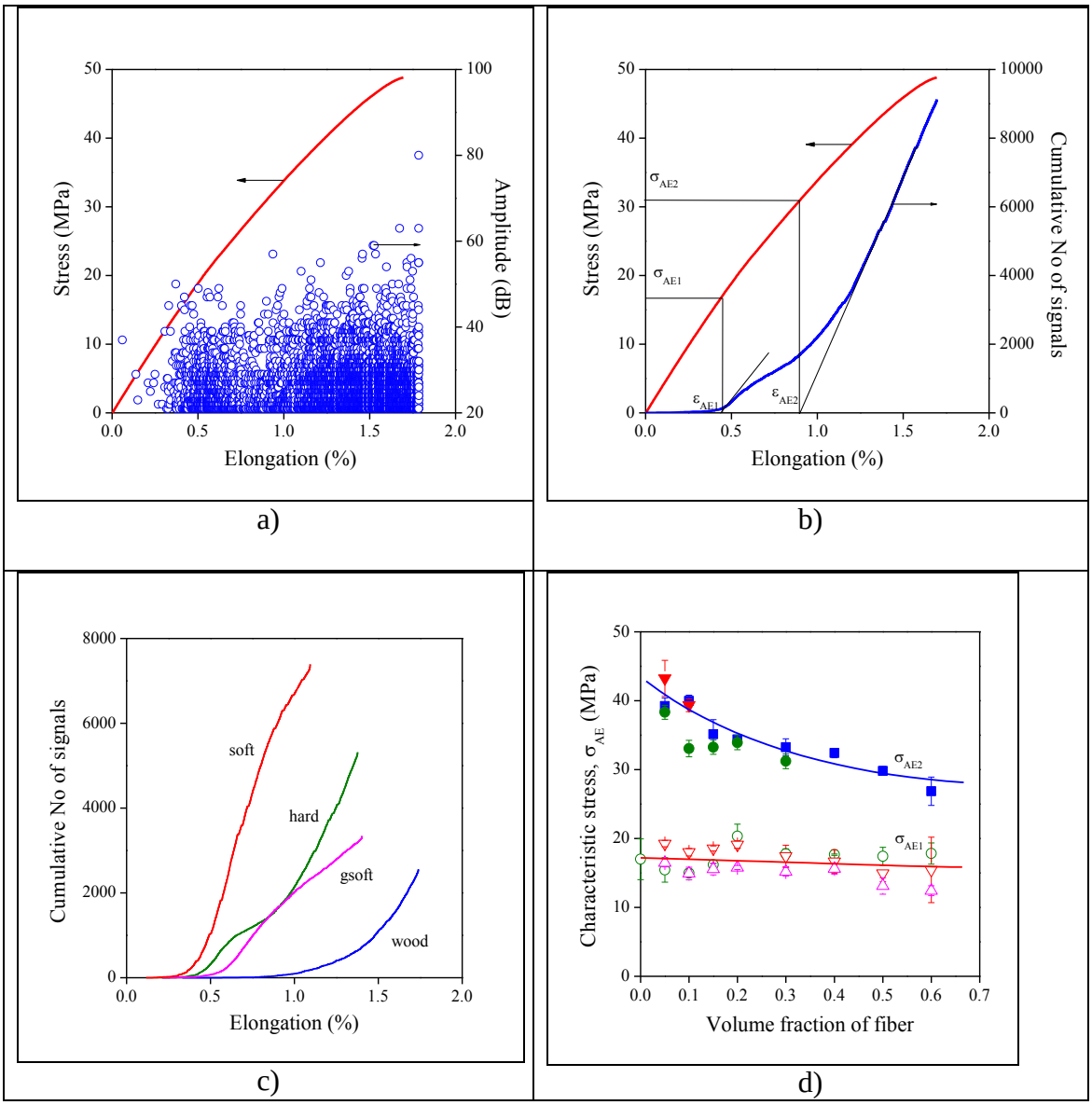
Stress (MPa)
Amplitude (dB)
Elongation (%)
a)
Stress (MPa)
Cumulative No of signals
σAE2
σAE1
εAE1
εAE2
Elongation (%)
b)
Cumulative No of signals
soft
hard
gsoft
wood
Elongation (%)
c)
Characteristic stress, σAE (MPa)
σAE2
σAE1
Volume fraction of fiber
d)

Faludi, Fig. 4

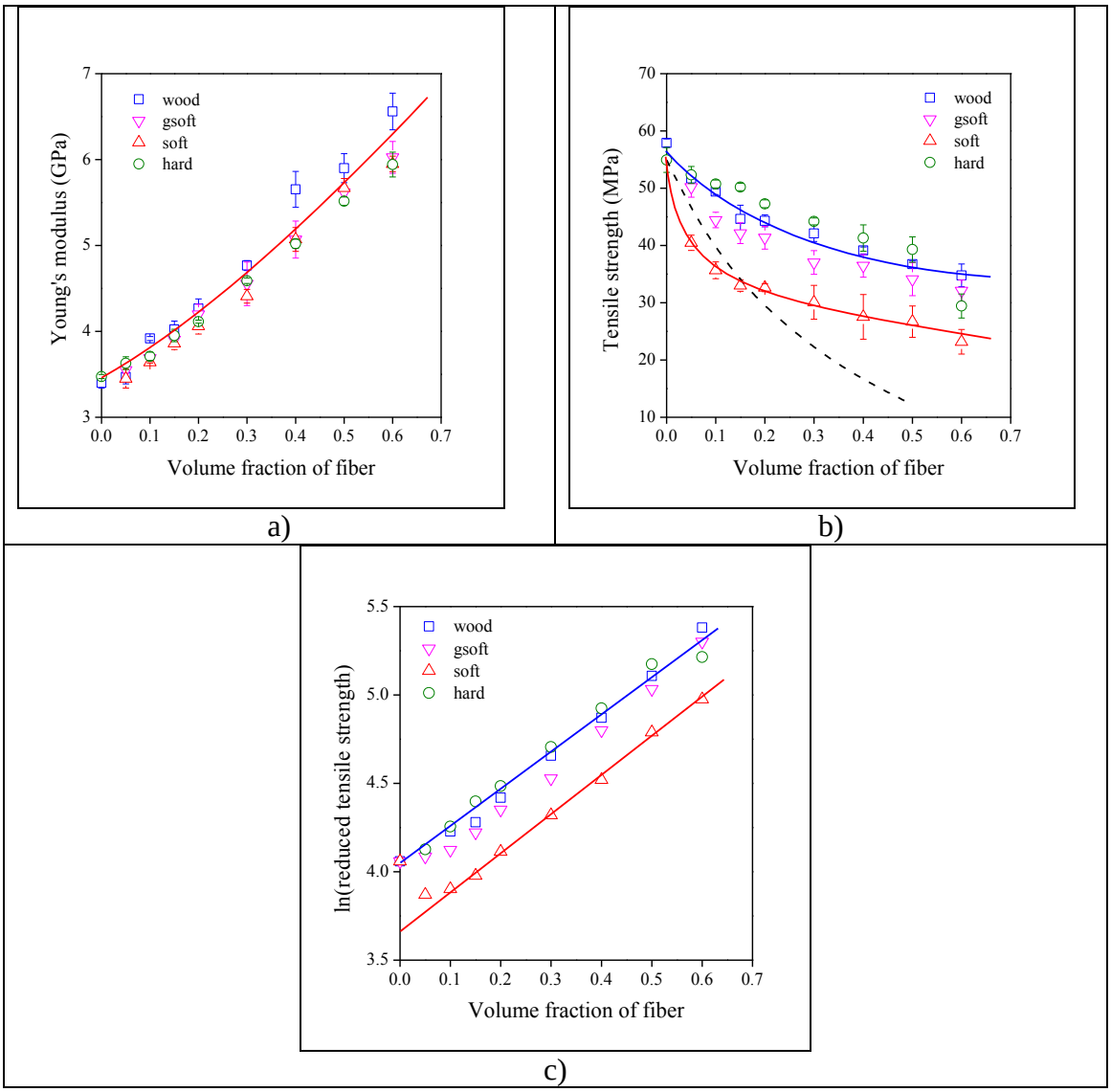
wood
gsoft
soft
hard
Young's modulus (GPa)
Volume fraction of fiber
a)
Tensile strength (MPa)
b)
ln(reduced tensile strength)
c)

Faludi, Fig. 5

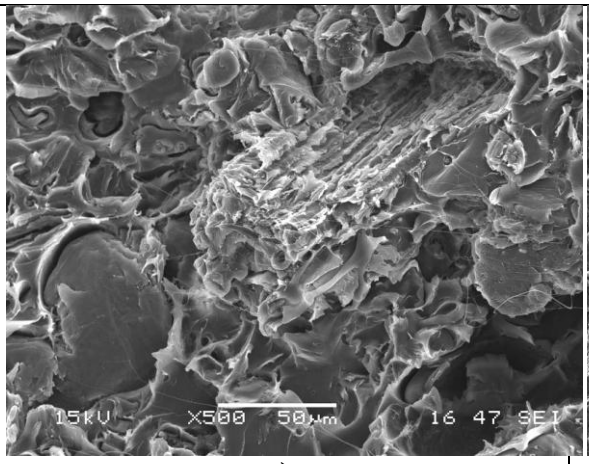

a)

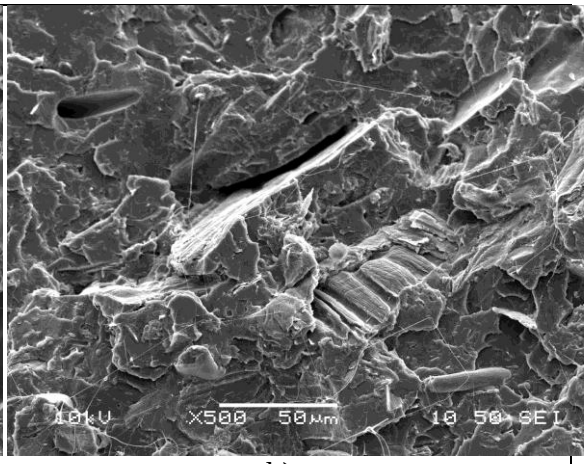

b)

c)

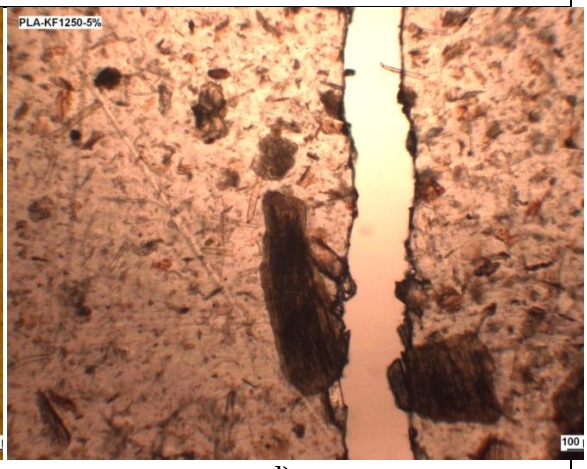

d)

Faludi, Fig. 6

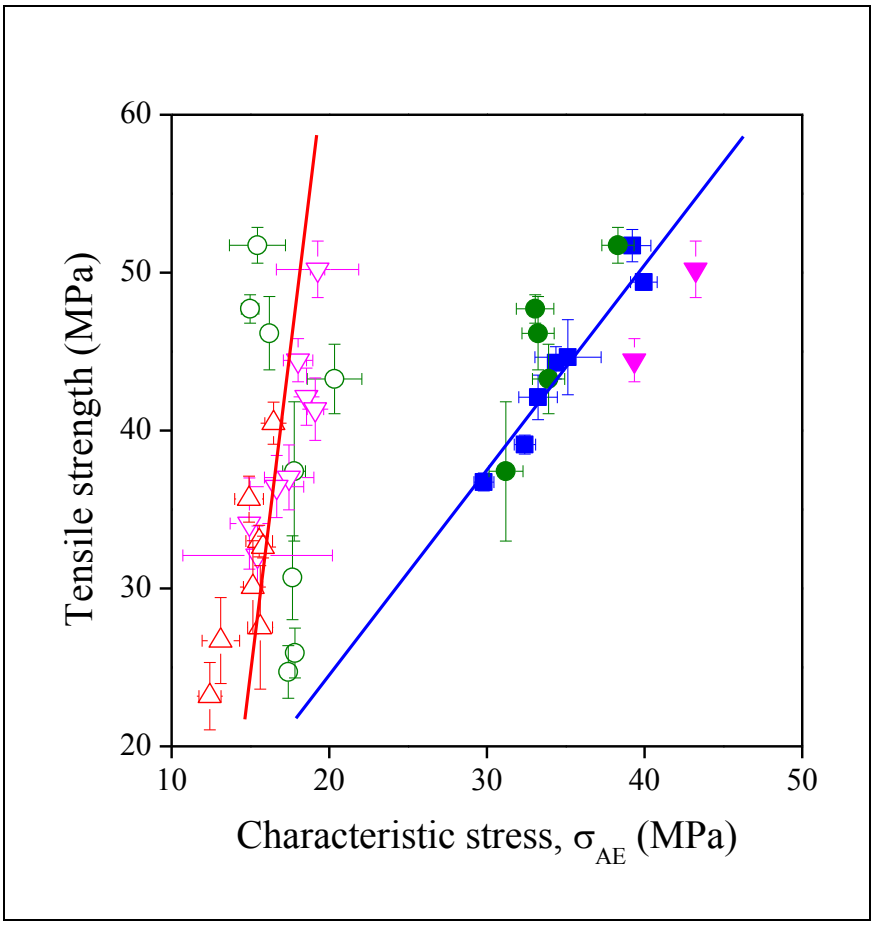
Tensile strength (MPa)
60
50
40
30
20
10
20
30
40
50
Characteristic stress, σ AE (MPa)

Faludi, Fig. 7

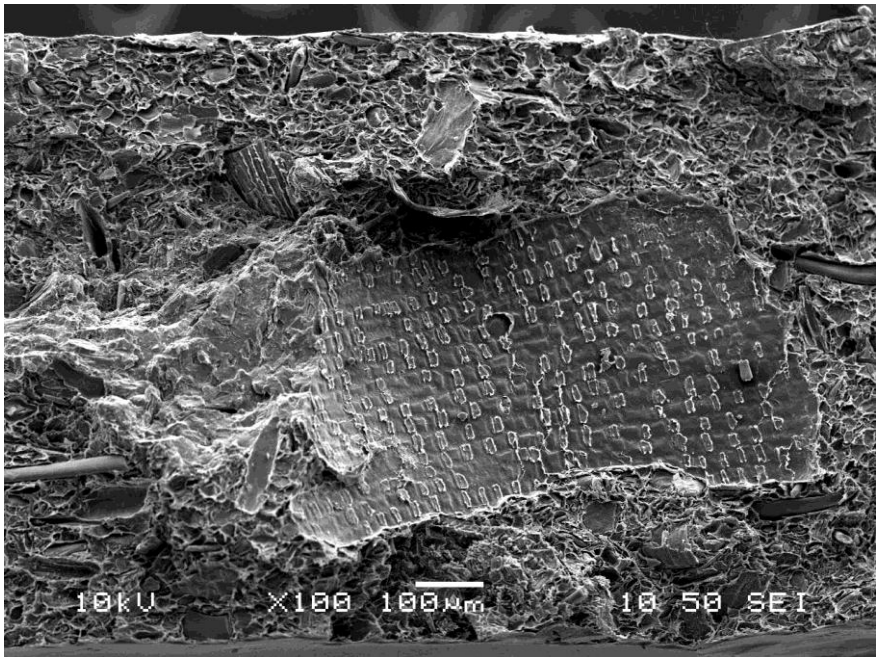

Faludi, Fig. 8

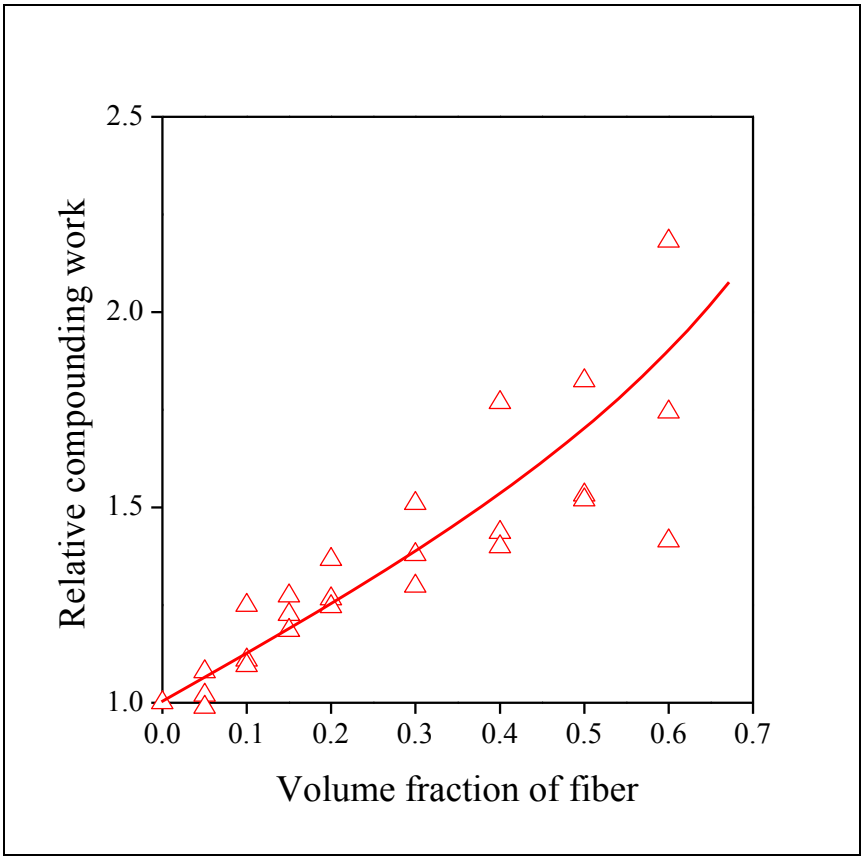
Relative compounding work
2.5
2.0
1.5
1.0
0.0
0.1
0.2
0.3
0.4
0.5
0.6
0.7
Volume fraction of fiber